Check for updates

Supramolecular Polymers

International Edition: DOI: 10.1002/anie.201905724
German Edition: DOI: 10.1002/ange.201905724

Revising Complex Supramolecular Polymerization under Kinetic and Thermodynamic Control

Jonas Matern, Yeray Dorca, Luis Sánchez, and Gustavo Fernández**

Keywords:
hierarchy · out-of-equilibrium systems · pathway complexity · self-assembly · supramolecular polymers

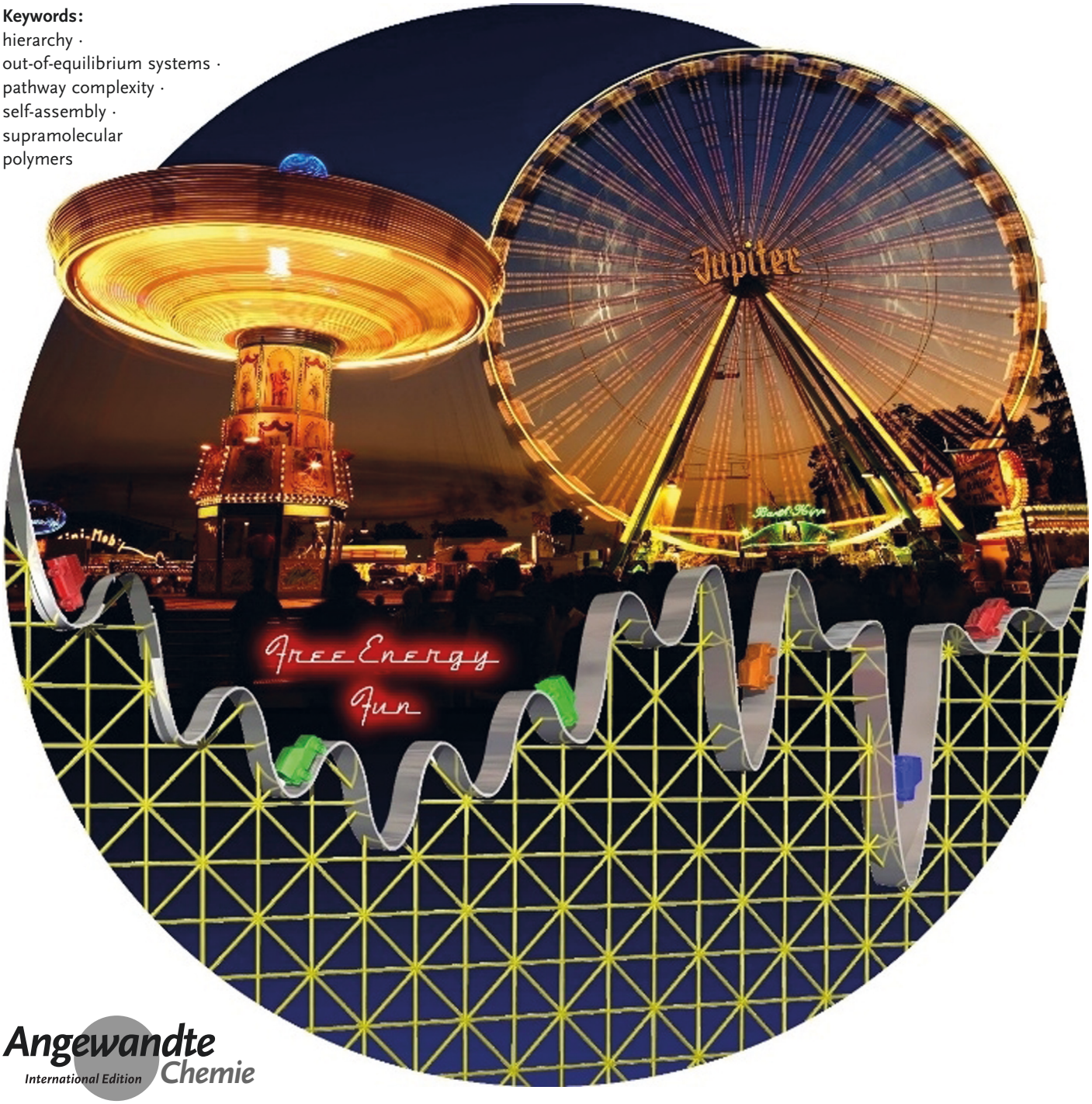

 © 2019 The Authors. Published by Wiley-VCH Verlag GmbH & Co. KGaA, Weinheim

Pathway complexity, hierarchical organization, out of equilibrium, and metastable or kinetically trapped species are common terms widely used in recent, high-quality publications in the field of supramolecular polymers. Often, the terminologies used to describe the different self-assembly pathways, the species involved, as well as their relationship and relative stability are not trivial. Different terms and classifications are commonly found in the literature, however, in many cases, without clear definitions or guidelines on how to use them and how to determine them experimentally. The aim of this Minireview is to classify, differentiate, and correlate the existing concepts with the help of recent literature reports to provide the reader with a general insight into thermodynamic and kinetic aspects of complex supramolecular polymerization processes. A good comprehension of these terms and concepts should contribute to the development of new complex, functional materials.

1. General Aspects of Supramolecular Polymerization

Inspired by the complexity and functionality of supramolecular systems in nature,[1] supramolecular polymers have emerged as promising smart nanomaterials with multiple potential applications ranging from optoelectronics to life sciences.[2] In contrast to classical polymers, the presence of reversible noncovalent interactions[3–5] provides access to outstanding functionalities, such as responsiveness to subtle stimuli or self-healing.[6] Supramolecular polymerization (SP) can be classified according to three different growth mechanisms into ring-chain, isodesmic, and cooperative polymerization, as previously reported in various excellent reviews.[3,4,7,8] Whereas ring-chain polymerization is limited to ditopic monomers, most examples of supramolecular polymers are described by either the (anti-)cooperative or isodesmic mechanisms.

The isodesmic or "equal K" model is characterized by an invariant value of the equilibrium constant of each association step during the monomer-to-aggregate transformation.[4,9] Cooperative (or "nucleated") SP occurs in two stages: initially a nucleus is formed with an association constant K_n, followed by an elongation process described by a new association constant K_e.[10] As a result of these two stages in cooperative SP, a critical concentration, temperature, or solvent composition has to be surpassed to initiate elongation. Both isodesmic and cooperative models have been used extensively to describe the SP of multiple compounds into a single, thermodynamically controlled aggregate.[7,8,11] However, self-assembled systems, particularly those governed by a cooperative mechanism, often exist as more than one single structure, which suggests that kinetic contributions should also be considered when analyzing self-assembly processes.[12–14] Thus, the parameter time also contributes drastically to the final outcome of the corresponding SP. Herein, we aim to classify, summarize, and relate existing concepts to promote a uniform terminology that is suitable to be generalized for all types of advanced supramolecular polymers. An in-depth comprehension of these terms and concepts should contribute to developing increasingly more advanced functional materials.

2. Competition of Thermodynamics versus Kinetics in SP

2.1. Early Manifestations of Multiple Aggregates from the Same Building Block

The existence of more than one final outcome in the self-assembly of a single molecule was a previously known phenomenon for various π-systems. As early as 1995, Boumann and Meijer reported on the stereomutation of thin films of a polythiophene derivative upon variation of the cooling rate.[15] Fast cooling yielded CD spectra with an opposite dichroic response compared to the slowly cooled samples. This stereomutation was attributed to the formation of kinetic structures (fast cooling) with opposite handedness to those formed under thermodynamic control (slow cooling).

In 2005, Ryu and Lee described the self-assembly of a bolaamphipilic molecule **1** (Figure 1).[16] In this work, the reversible aqueous coassembly of cylindrical structures of **1** and a complementary rod-coil-rod molecule was analyzed. Strikingly, the desired cylindrical micelles of **1** were not obtained directly upon SP, but instead spherical micelles were formed. However, over a period of four weeks, the micellar kinetic assemblies transformed into the thermodynamically stable cylindrical architectures, as evidenced by dynamic light scattering (DLS) and transmission electron microscopy (TEM, Figure 1 b,c).

More recently, Rybtchinski and co-workers reported the amphiphilic Pt^{II} complex **2** that self-assembles into three different aggregates depending on the selected percentages of water and THF (Figure 2).[17] At high water contents (95:5),

[*] J. Matern, Prof. Dr. G. Fernández
Organisch-Chemisches Institut
Westfälische Wilhelms-Universität Münster
Corrensstrasse 40, 48149 Münster (Germany)
E-mail: fernandg@uni-muenster.de
Y. Dorca, Prof. Dr. L. Sánchez
Departamento de Química Orgánica
Facultad de Ciencias Químicas
Universidad Complutense de Madrid
28040 Madrid (Spain)
E-mail: lusamar@quim.ucm.es
The ORCID identification number for some of the authors of this article can be found under: https://doi.org/10.1002/anie.201905724.

© 2019 The Authors. Published by Wiley-VCH Verlag GmbH & Co. KGaA. This is an open access article under the terms of the Creative Commons Attribution Non-Commercial License, which permits use, distribution and reproduction in any medium, provided the original work is properly cited and is not used for commercial purposes.

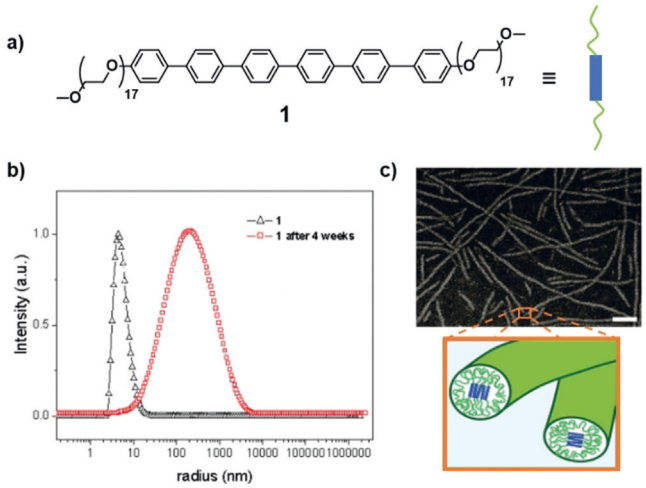

Figure 1. a) Chemical structure of amphiphile **1**. b) Time-dependent DLS measurement showing the transformation of initially formed spherical micelles into cylindrical micelles. c) TEM image of an aged solution showing cylindrical micelles. Adapted from Ref. [16] with permission. Copyright 2005 American Chemical Society.

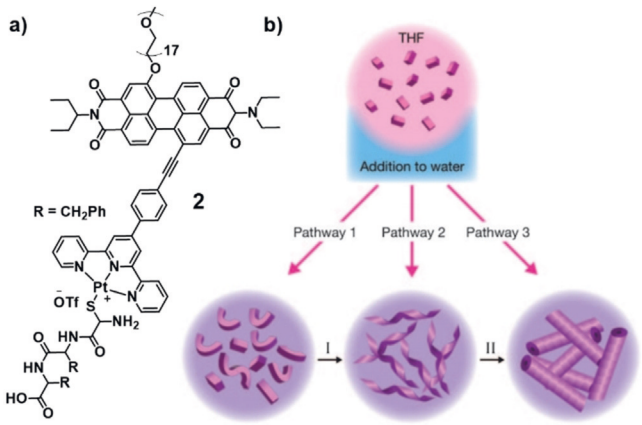

Figure 2. Chemical structure of amphiphilic Pt^{II} complex **2** and its pathway-dependent self-assembly. Adapted from Ref. [17] with permission. Copyright 2011 Wiley-VCH.

cryo-TEM revealed highly curved, fibrous assemblies with a weak CD response that does not change over time (Figure 2, pathway 1). Increasing the THF percentage to 20% induces a marked CD signal that originates from helical, fibrous structures (pathway 2). Another distinct CD pattern corresponding to tightly packed, straight nanofibers was obtained in 70:30 water/THF mixtures after 70 h (pathway 3). The authors concluded that the aggregates formed at a high water content are kinetic species that are unable to convert into the thermodynamic structure because of strong hydrophobic interactions. In contrast, assemblies prepared in 80:20 or 70:30 mixtures can equilibrate to the thermodynamic product. Interestingly, depending on the preparation method, all three structures could be isolated under equal final conditions (95:5 water/THF, $c = 1\text{x}10^{-4}$, RT).

This "pathway-dependent" self-assembly, as denoted by the authors, marked a milestone in exploiting kinetic control to tune the outcome of SP.

2.2. The Concept of Pathway Complexity

Although the insufficiency of a mere thermodynamic assessment had been recognized for more than a decade, it was not until 2012 that Meijer and co-workers systematically unraveled the competition between kinetics and thermody-

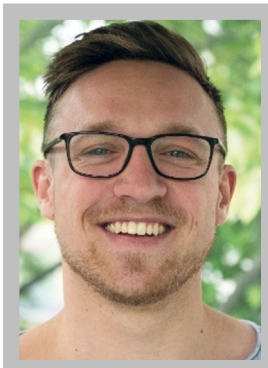

Jonas Matern received his B.Sc. and M.Sc. from the Ruprecht-Karls-Universität Heidelberg (2016) and Westfälische-Wilhelms Universität Münster (WWU, 2018), respectively. He is currently working in the group of Prof. Gustavo Fernández at the WWU. His work focuses on the systematic study of the factors governing supramolecular polymerization in metal-containing systems.

Luis Sánchez has been professor of Organic Chemistry since 2002 and leads the "Supramolecular Polymers" group at the Universidad Complutense de Madrid. His research interests focus on realizing new supramolecular polymers, especially helical aggregates, to develop functional materials.

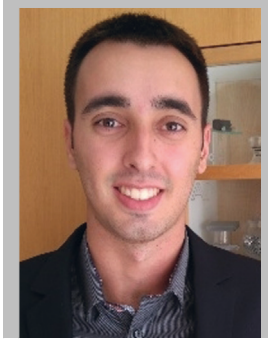

Yeray Dorca obtained his B.Sc. in Chemistry (2015) and his M.Sc. in Organic Chemistry (2016) at the Universidad Complutense de Madrid (UCM). He joined the group of Prof. Luis Sánchez as a PhD student, working on the self-assembly of nonplanar aromatic molecules.

Gustavo Fernández has been professor of Organic and Supramolecular Chemistry at the WWU (Münster) since 2015, where he heads a research group working on self-assembled π-systems. His research focuses on understanding the mechanistic aspects involved in the supramolecular polymerization of functional, metal-containing and BODIPY-based systems.

 © 2019 The Authors. Published by Wiley-VCH Verlag GmbH & Co. KGaA, Weinheim

namics in SP. Following their seminal work on the nucleated SP of a chiral oligophenylene vinylene (OPV) derivative **3**,[18] the authors examined the existence of competing pathways. In particular, new kinetic experiments and calculations were introduced to shed light onto the interplay between thermodynamic and kinetic pathways, in terms of the influence of concentration, temperature, and solvent composition.[19,20]

(*S*)-Chiral OPV **3** self-assembles into thermodynamically stable, *M*-type helices upon slow cooling (1 K min^{-1}) from the molecularly dissolved state. In contrast, a fast temperature drop to 273 K leads to a mixture of *M*-type and kinetically favored *P*-type helices. Stopped-flow CD experiments, in which a chloroform solution of **3** was injected into a large volume of a poor solvent (methylcyclohexane, MCH), revealed an initial formation of the kinetic *P*-type aggregates at high concentrations (Figure 3b). The appearance of this "off-pathway" assembly caused an increase in the time required to assemble 50% of the monomers (lag time, t_{50}) upon increasing the concentration. This behavior could be explained by assuming that the *P*- to *M*-helix transition occurs through a disassembly into the monomer (Figure 3c).

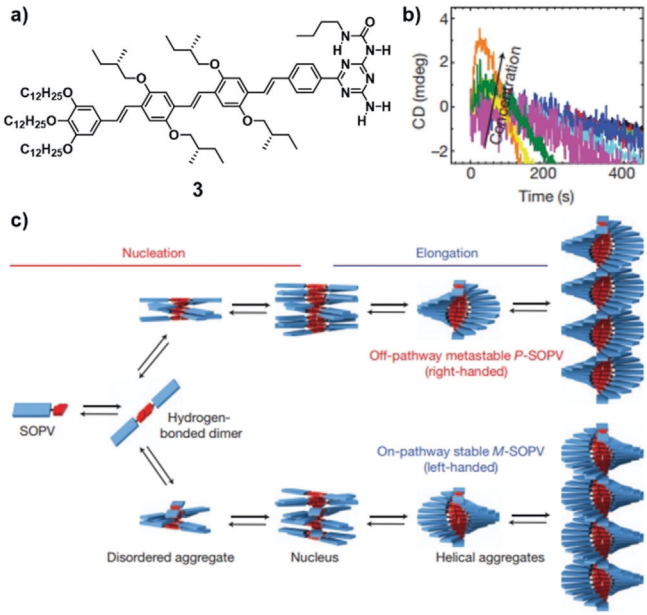

Figure 3. a) Chemical structure of **3**. b) Plots of CD signal versus time in stopped-flow kinetic experiments. c) Schematic illustration of the competitive aggregation pathways of **3**. Adapted from Ref. [20] with permission. Copyright 2012 Springer Nature.

Hence, the formation of the kinetic polymers sequesters the monomers, thus lowering the concentration of free monomers able to engage in the thermodynamic pathway and decelerating the formation of the *M*-helix. Simulations could correlate these findings to a slightly more stable nucleus for the *P*-helix, whereas the *M*-helix is more stable in the elongation regime. Based on these findings, the authors introduced the term pathway complexity, which was already used for proteins, to describe the appearance of different aggregation pathways that are in competition for the monomer.[21]

Subsequent to this pioneering work, the focus in SP shifted from a pure thermodynamic view towards increasing attention to kinetic aspects. Pathway complexity has in the meanwhile become a frequently used term in systems exhibiting more than a simple monomer to aggregate transformation.

2.3. Concepts Used To Describe Thermodynamic and Kinetic Aspects of Complex SP

The increasingly detailed investigations on pathway complexity phenomena prompted the emergence of a multitude of concepts and terminologies to describe the SP processes and species. Some of these concepts/classifications have been used interchangeably in the literature, which makes a clear differentiation between particular subsets difficult. In the following, we provide our understanding of the concepts commonly used to describe complex SP phenomena. In particular, we aim to classify, summarize, relate, and expand existing concepts to promote a uniform terminology that can be generalized for all types of advanced SP systems. The concepts illustrated in Figure 4 will be addressed in a general manner in this section with the help of representative examples from the literature. In particular, energy landscapes under a given set of conditions (i.e. concentration, temperature, solvent composition) will be used to distinguish the different self-assembled structures encountered in a system.

2.3.1. Dissipative versus Non-dissipative

When considering the self-assembly of a monomer (M) into ordered nanostructures (i.e. moving along the energy landscape of the system), the species that are stable on an experimentally observable time scale represent minima of the respective potential energy curve. Thus, their instantaneous transformation into a lower-energy species is retarded by a non-negligible activation barrier. These states are called non-dissipative states (states A and B in Figure 4a).[22] Dissipative or transient states, in contrast, (T in Figure 4a) have a very low or no activation barrier to hinder a further descent in the energy landscape.[23] Therefore, the continuous input of energy of some kind (i.e. a fuel) is required to prevent relaxation into the next energy minimum.[24] The corresponding far-from-equilibrium structures degrade when the fuel supply is stopped. At this point, we refer the reader to a handful of excellent reports on dissipative systems,[23,25] as this Minireview will focus on non-dissipative systems.

2.3.2. Equilibrium versus Non-equilibrium

The thermodynamic equilibrium is represented by the global energy minimum of the energy landscape (B in Figure 4a). A system in this condition may still be dynamic, with monomers continuously equilibrating between solution and aggregates, but the overall system does not change over time. As the energy landscape is dependent on parameters such as concentration, temperature, and solvent composition, the equilibrium species may vary for a different set of

 © 2019 The Authors. Published by Wiley-VCH Verlag GmbH & Co. KGaA, Weinheim

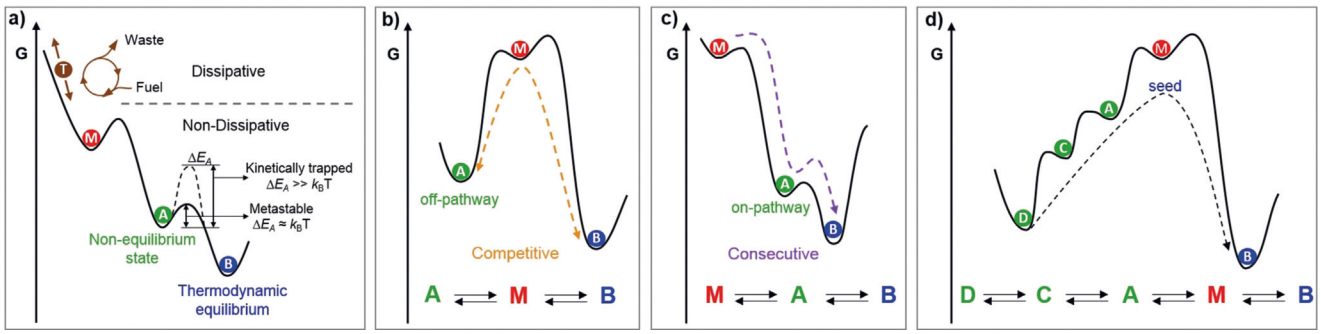

Figure 4. Energy landscapes illustrating the different concepts for pathway/aggregate characterization: a) dissipative versus non-dissipative and equilibrium versus non-equilibrium states; b) competitive pathways; c) consecutive pathways; d) system of higher complexity with a hierarchical kinetic pathway and the possibility of living SP by a seeded-growth approach.

conditions. However, the way in which it is reached has no influence on the final equilibrium structure.[24,26] Any other species different from the thermodynamically stable one is a kinetic, non-equilibrium structure. Recent advances in the field have shown that time is a key parameter that must be considered when assessing the equilibrium versus non-equilibrium nature of different states. Kinetic, non-equilibrium structures are prone to spontaneously convert into the equilibrium state over time or by application of some kind of stimulus that aids in overcoming the activation barrier to ease into the global minimum.

2.3.3. Metastable versus Kinetically Trapped

The magnitude of this activation barrier can give rise to a differentiation of kinetic species into either metastable or kinetically trapped species.[22] Energy barriers that can be overcome at room temperature (i.e. no greater than k_BT) exist for metastable structures. These structures transform to more stable species within an experimentally observable time scale, which often ranges from minutes to several months. Kinetically trapped states, in contrast, reside in a local energy minimum if not pushed over the energy barrier by some external stimulus.[24] Nevertheless, the lack of explicit experimental means to differentiate the two states has resulted in these two terms having been used interchangeably in the literature. However, for the assessment of the properties of a SP system, the exact categorization of each kinetic species as either metastable or kinetically trapped is not necessary, in our opinion. The most crucial characteristic for controlling SP through kinetic species, namely retardation of the spontaneous self-assembly of the thermodynamic polymer, is guaranteed in both cases.

2.3.4. On- versus Off-Pathway Species, Consecutive and Competitive Pathways

The occurrence of multiple pathways in SP prompted the use of the terms "on-pathway" and "off-pathway" aggregates. In many cases, the terms are used as synonyms for thermodynamic and kinetic species, respectively. However, there are examples of on- and off-pathway aggregates that cannot be accurately described by this simple definition.[27] More precisely, the terms refer to the final outcome of an individual branch of an energy landscape. This becomes apparent when inspecting the archetypal energy landscape of a more complex system (Figure 4d).

Along the kinetic pathway, A is an on-pathway aggregate towards species D. On the other hand, A is an off-pathway aggregate with respect to thermodynamic species B. Thus, it is crucial to define the state of reference when using the expressions on- and off-pathway.

In this context, even though the terms sequential and parallel have been referred to in the literature,[28] we suggest the terms "consecutive" and "competitive" as a more intuitive designation to describe the relationship of the individual pathways (Figures 4b,c). Species or pathways that can only be transformed into each other through disassembly into the monomer are competitive (Figure 4b). When a species converts into another one directly, for example, by means of structural rearrangements or formation of higher ordered architectures (e.g. clustering), then the pathway is consecutive (Figure 4c). In the case of the most simple, three-state energy landscape (Figures 4b,c), the classification of off- and on-pathway for state A with respect to thermodynamic species B coincides with the competitive/consecutive characterization of the pathways.[28]

The key experiment to distinguish the two cases is the time-dependent interconversion between the respective polymeric species at different concentrations. If the transformation is accelerated upon increasing the concentration, that is, the time required for the transition to be completed (lag time) is shorter, a consecutive pathway occurs. On the other hand, if the lag time increases with increasing concentration, competitive pathways exist, as the less-stable species has to be transformed into free, aggregation-active monomers prior to assembly into the more stable aggregate. Other distinctive features of competitive and consecutive systems will be mentioned in the following section by describing selected examples from the literature.

2.3.5. Hierarchy

The concept of hierarchy was derived from protein folding, which proceeds in a series of successive steps, that is, hierarchical levels (primary to quaternary structure).[29] A

 © 2019 The Authors. Published by Wiley-VCH Verlag GmbH & Co. KGaA, Weinheim

hierarchical process is defined by consecutive assembly levels, where a more advanced macroscopic organization is added at each stage, while keeping the substructure motifs of the precedent levels. In most cases, a correlation between the hierarchical level and the forces governing its structure exists. The stronger interactions dictate the formation of the first aggregation step, while the strength of these forces diminishes when approaching the lowest energy state. Usually, a hierarchical SP is directly related to a consecutive pathway.

2.3.6. Living/Seeded Supramolecular Polymerization

Inspired by the work on crystallization-driven self-assembly by Manners and co-workers,[30] and in analogy to classical chain-growth polymerization, living supramolecular polymerization (LSP) has been exploited as a tool to control the length and polydispersity in SP. This approach takes advantage of kinetic species, which serve as a monomer reservoir. The metastable or kinetically trapped species are transformed to aggregates of lower energy when certain stimuli are applied to the inactive species (Figure 4d). A prerequisite for LSP is the retardation of the spontaneous self-assembly of the thermodynamically favored species.[31] The terms living and seeded SP are often used interchangeably in the current literature. Our view on this subject is that the most appropriate terminology would be "LSP by seeded growth" or "seed-mediated LSP", as the seeds are the specific stimuli that initiate SP with living character. LSP has also been achieved by an initiator molecule-induced approach by the group of Aida,[32] as will be outlined in Section 2.5.

Before moving on to illustrate these concepts using selected literature examples, it should be mentioned that such phenomena are often combined or occur simultaneously. For example, hierarchical levels can be encountered along both the kinetic and thermodynamic pathways. This also applies to metastable or kinetically trapped species (Figure 4d). Furthermore, those species could be inactive aggregates or "dormant" monomers (e.g. through intramolecular H-bonding[33–38]). In the following, we will systematically move from purely consecutive to purely competitive systems to finally show complex systems exhibiting several of the aforementioned phenomena. For more detailed information about the key experiments needed to identify all the concepts described in this section, the reader is referred to the original manuscripts.

2.4. Consecutive Pathways

An archetypal example of a system exhibiting consecutive pathways is the hierarchical supramolecular polymerization of a series of merocyanine dyes reported by Würthner and co-workers (Figure 5).[12,14,39] Initially, two dye units of **4** form antiparallel dimer aggregates (D-aggregates) through dipolar interactions and these aggregates organize into single fibrils with a helical conformation. Six of the resulting helical fibrils further grow into densely packed rods with the alkoxy chains pointing outwards (H-aggregates). At higher concentrations, gelation occurs as a result of inter-rod interdigitation of the

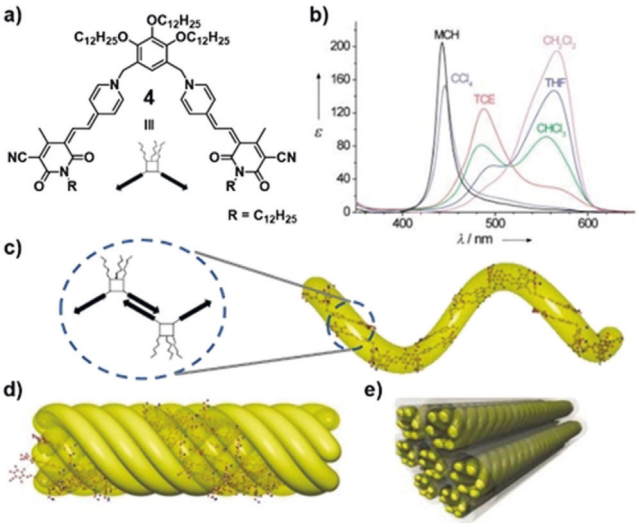

Figure 5. a) Structure of merocyanine dye **4** and b) its solvent-dependent UV/Vis spectra. Hierarchical self-assembly by dimerization and subsequent growth into c) helical fibrils that d) form rods that e) ultimately intertwine. Adapted from Ref. [39] with permission. Copyright 2003 Wiley-VCH.

paraffinic side chains (Figures 5c–e). The stabilization of the different hierarchical states by variation of the concentration and solvent (i.e. change in the energy landscape) was successfully exploited to isolate monomeric as well as D- and H-aggregated species. In CH_2Cl_2, **4** is molecularly dissolved with an absorption maximum at $\lambda = 570$ nm, while a sharp blue-shifted band, originating from highly organized H-type aggregates, is evident in apolar MCH (Figure 5b). In solvents of intermediate polarity, such as tetrachloroethane (TCE), the previously mentioned and less hypsochromically shifted D-band, is observed. In the appropriate solvent combination (42:58 MCH/THF), full transition from monomers to elongated H-aggregates via the formation of D-aggregates was achieved by variation of the temperature, thus indicating the consecutive, hierarchical nature of the self-assembly. Additional proof of the hierarchical self-assembly was achieved with chiral congeners of **4**, where the D- to H-aggregate transformation could be monitored over time by CD spectroscopy.[12,14]

Yagai and co-workers reported the hierarchical SP of a V-shaped azobenzene-based photochromic system **5** (Figure 6).[40] Cooling monomer solutions of **5** in MCH leads to a weak bisignate Cotton effect between 44 °C and 20 °C (inset Figure 6b). These spectroscopic changes were attributed to the formation of H-type nanotoroids driven by hydrogen bonding, as confirmed by AFM (Figure 6c), TEM, and FTIR spectroscopy. Further cooling causes the appearance of several new, intense dichroic signals (Figure 6b). This reversible transition is ascribed to the subsequent organization of the toroids into chiral nanotubes through π-stacking (Figure 6d). Ageing of the solution at 0 °C induces a subsequent stacking and twisting into supercoiled fibrils that eventually intertwine to form chiral double helices (Figure 6e).

Ajayaghosh and co-workers recently reported another remarkable example of consecutive assemblies involving

 © 2019 The Authors. Published by Wiley-VCH Verlag GmbH & Co. KGaA, Weinheim

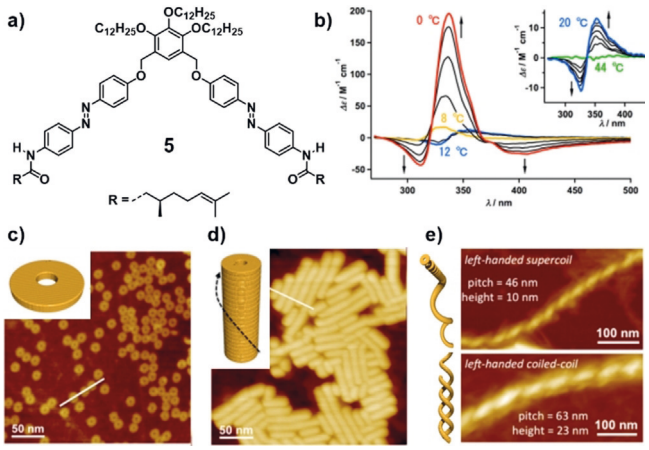

Figure 6. a) Structure of photochromic unit **5** and b) corresponding CD spectra recorded upon hierarchical SP into c) nanotoroids, d) nanotubes, and e) eventually chiral single and double helices, as observed by AFM. Adapted from Ref. [40] with permission. Copyright 2012 American Chemical Society.

exceptional chiroptical transitions depending on the hierarchy level.[41] Oligophenylene-ethynylene (OPE) derivative **6** self-assembles into chiral helices whose handedness is inverted when they coil into superhelical structures (Figure 7). Disassembly curves of superhelices, and their single-helix precursors could prove the direct, consecutive interconversion of the two species. The convergence of the temperature-induced depolymerization curve of *P*-superhelices into the one obtained for single *M*-helices under equal conditions (*n*-decane, $c = 5\text{x}10^{-5}$ M) perfectly corroborated their hierarchical relationship (Figure 7b).

The appearance of assembly or disassembly curves with two or more transitions during variable-temperature (VT) spectroscopic measurements has been observed in several systems exhibiting consecutive pathways. In particular, examples of partially fluorinated benzenetricarboxamides[42] and N-annulated perylenes[35,37] show three regimes in the respective VT-UV/Vis experiments that correspond to nucleation, elongation, and, finally, bundling into thicker aggregates.

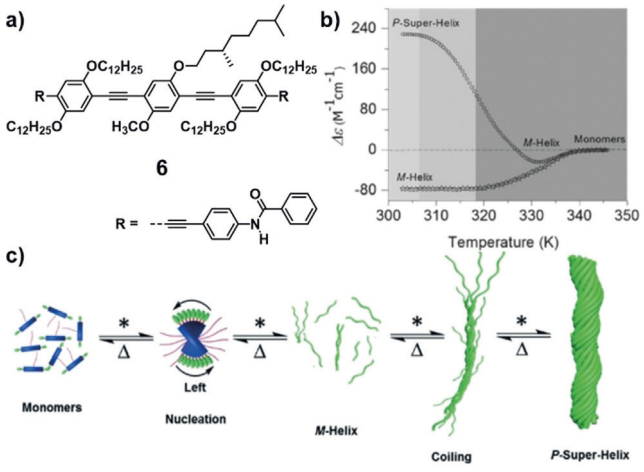

Figure 7. a) Chemical structure of OPE **6** and c) its hierarchical self-assembly. b) Temperature-induced disassembly curve of *P*-type superhelices that converges with the curve obtained for *M*-type helices. Adapted from Ref. [41] with permission. Copyright 2017 Wiley-VCH.

2.5. Competitive Pathways

Competitive pathways occur when two or more self-assembled structures compete for the monomer, that is, interconversion is only possible by disassembly and subsequent reassembly into a different structure. One of the most prominent examples of competitive pathways was the previously described (*S*)-OPV **3**, which forms two species of opposite helicity.[20]

In 2014, Ogi et al. reported the first example of LSP when investigating a Zn porphyrin (ZnP) that self-assembles through two competitive pathways (Figure 8).[43] Upon cooling monomer solutions of **7** in MCH, nanoparticles with a slipped J-type stacking were formed in an isodesmic fashion (step 1 in Figures 8b,c). No thermal hysteresis, that is, discrepancy between the cooling and heating curves in a successive cycle of assembly and disassembly, could be detected for this process. Such hysteresis is a distinct characteristic of a competing species that sequesters free monomers.[33–37] However, over the course of several days, the J-aggregates transformed to H-type fibers (step 2). The lag time (t_{50}) for this transformation was found to increase with the concentration of **7**. This suggested that the transformation proceeds via free monomer, thereby establishing the nanoparticles as off-pathway aggregates.

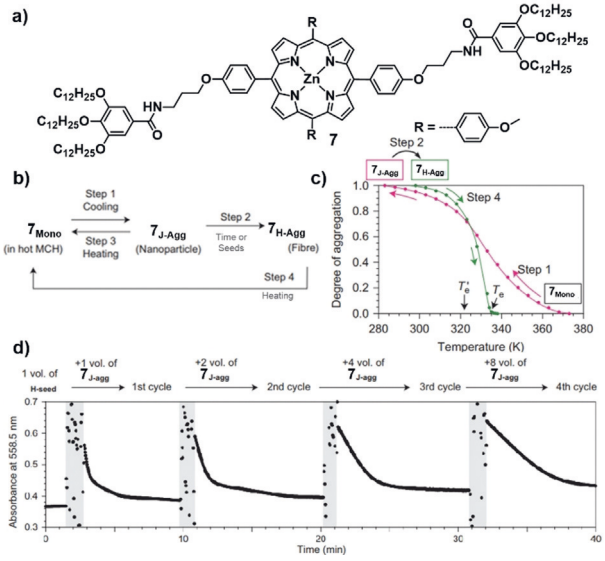

Figure 8. a) Chemical structure of **7** and b) its competitive J- versus H-type aggregation. c) Cooling (pink) and heating (green) curves for the two possible pathways. d) Four-cycle LSP through seeded growth from J- to H-aggregates. Adapted from Ref. [43] with permission. Copyright 2014 Springer Nature.

The cooperative mechanism governing the formation of $\mathbf{7}_{\mathbf{H\text{-}agg}}$ was unveiled by monitoring the dissociation process upon heating (step 4). Notably, the elongation temperature T_e

 © 2019 The Authors. Published by Wiley-VCH Verlag GmbH & Co. KGaA, Weinheim

for $\mathbf{7}_{\mathbf{H\text{-}agg}}$ in this experiment (heating→thermodynamic control) was higher than the value predicted by the cooperative model without interference of the off-pathway aggregate ($T_{e'}$→hysteresis; Figure 8c). This can be explained by a lower concentration of free monomer that can form nuclei of $\mathbf{7}_{\mathbf{H\text{-}agg}}$ as a result of the formation of the off-pathway $\mathbf{7}_{\mathbf{J\text{-}agg}}$. Thus, the appearance of $\mathbf{7}_{\mathbf{J\text{-}agg}}$ has a direct impact on the formation of the thermodynamic species by inhibiting the spontaneous polymerization of $\mathbf{7}_{\mathbf{H\text{-}agg}}$. This analogy to nucleated amyloid fibril formation in nature[44] inspired the authors to probe the possibility of LSP for the first time. Indeed, the addition of seeds of $\mathbf{7}_{\mathbf{H\text{-}agg}}$ (obtained by sonication) to $\mathbf{7}_{\mathbf{J\text{-}agg}}$ caused an immediate J→H transition, whose kinetics depend on the $[\mathbf{7}_{\mathbf{J\text{-}agg}}]/[\mathbf{7}_{\mathbf{H\text{-}seed}}]$ ratio. Repeated cycles of mixing equally concentrated solutions of $\mathbf{7}_{\mathbf{J\text{-}agg}}$ and $\mathbf{7}_{\mathbf{H\text{-}seed}}$ corroborated the living nature of the observed process, as the rate was diminished by half in each cycle (Figure 8d).

A particularly relevant approach to broaden the scope of LSP consists of the use of monomers that can be trapped in a "dormant" state through the formation of intramolecular hydrogen bonds, which retards spontaneous self-assembly. This is the case for PBI **8** reported by Würthner and co-workers, in which the stabilization of a dormant monomer through amide/imide intramolecular hydrogen bonding prevents self-nucleation (Figure 9a).[34] A clear hysteresis in both pure toluene and MCH/toluene (2:1) was observed when comparing the cooling and heating cycles (Figure 9b). The kinetic dormant state can be subsequently used as a monomer reservoir for seed-induced LSP, thereby demonstrating that it is not only kinetic aggregates that can serve as monomer feedstock in controlled SP.

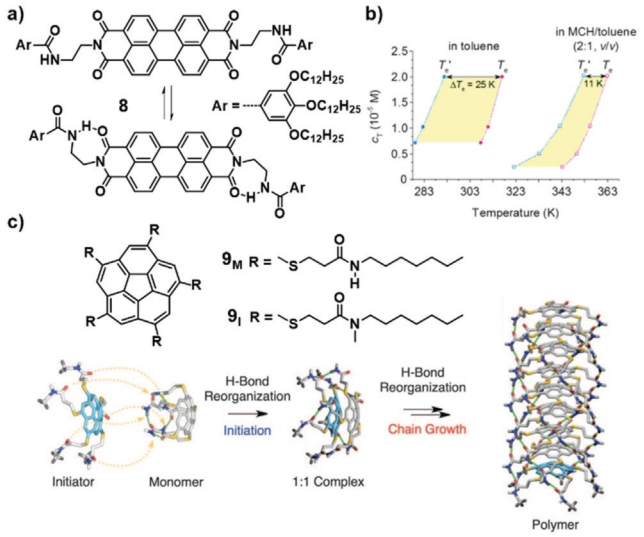

Figure 9. a) Chemical structure of PBI **8** and the equilibrium between the active and dormant conformation. b) Thermal hysteresis during the SP of **8** in toluene and MCH/toluene (2:1 v/v). c) Chemical structures of corannulene derivatives $\mathbf{9}_{\mathbf{M}}$ (monomer) and $\mathbf{9}_{\mathbf{I}}$ (initiator). A schematic representation of LSP of dormant $\mathbf{9}_{\mathbf{M}}$ initiated through addition of $\mathbf{9}_{\mathbf{I}}$ inducing H-bond reorganization is also shown. Adapted from Ref. [34] with permission. Copyright 2015 American Chemical Society and from Ref. [32]. Copyright 2015 AAAS.

Aida and co-workers reported on the initiator molecule-induced LSP of a bowl-shaped corannulene derivative ($\mathbf{9}_{\mathbf{M}}$) with five amide-appended thioalkyl side chains. This molecule remains in a cage-like "dormant" monomer conformation as a consequence of the formation of an array of intramolecular hydrogen bonds in MCH at 25 °C (Figure 9c).[32] Increasing the temperature allows $\mathbf{9}_{\mathbf{M}}$ to adopt an open conformation that enables SP, thus showing the competitive character of the closed conformation (dormant monomer) and polymer. Based on these observations, the authors realized LSP by the addition of the N-methylated derivative $\mathbf{9}_{\mathbf{I}}$, a polymerization initiator that is unable to adopt the closed conformation (Figure 9c). Molecules of $\mathbf{9}_{\mathbf{I}}$ act as hydrogen-bond acceptors, inducing reorganization in the dormant monomers and thus initiating LSP.

Recently, our groups reported an example of a supramolecular polymer that exists as two concomitant, stable, polymorphic structures. VT-UV/Vis and AFM experiments showed that OPE-based Pt^{II} complex **10** forms two competing aggregates in MCH depending on the cooling rate and concentration (species **A** and **B** in Figure 10b).[45] Polymorph **A** with a slipped molecular arrangement stabilized by N–H···Cl–Pt interactions is obtained at high rates (2 K min^{-1}) through an isodesmic mechanism. The cooperative formation of **B**, characterized by a pseudoparallel stacking driven by N–H···O_{alkoxy} hydrogen bonding, is preferred at lower cooling rates (0.1 K min^{-1}). Under intermediate conditions, the two species form concomitantly without interconversion, even

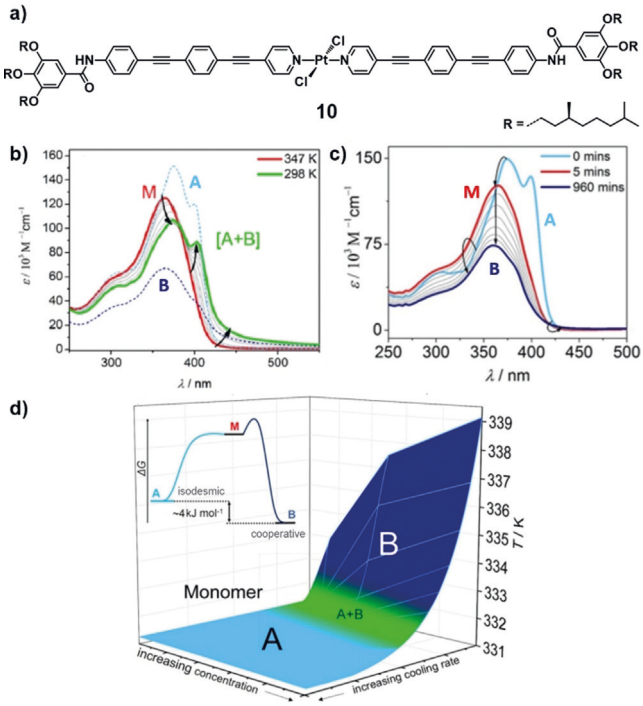

Figure 10. a) Chemical structure of OPE-Pt^{II} complex **10**. b) UV/Vis spectra of the monomer (M), as well as concomitant aggregates (**A** and **B**). c) Time-dependent UV/Vis spectra showing the transformation of **A** into **B** via **M**. d) Phase diagram and energy landscape showing the competitive pathways. Adapted from Ref. [45] with permission. Copyright 2019 American Chemical Society.

 © 2019 The Authors. Published by Wiley-VCH Verlag GmbH & Co. KGaA, Weinheim

after prolonged time. This demonstrates the minor energy difference between the two species, which was calculated to be 4 kJ mol^{-1}. The **A**→**B** transformation could only be realized upon annealing solutions of kinetic species **A** at elevated temperatures (Figure 10c). The corresponding UV/Vis studies showed that disassembly of **A** into monomers occurs prior to reassembly into polymorph **B**, thus showing that **A** is a competitive, off-pathway aggregate with respect to **B**. Close scrutiny of the system allowed an experimental phase diagram to be established that can be used to predict the outcome of the SP (Figure 10d).

2.6. Systems of Higher Complexity

All of the previously described systems were characterized by an energy landscape consisting of only one thermodynamic and one kinetic pathway. However, analysis of SP can become more challenging in those cases where more than one kinetic pathway exists.

In this context, the groups of De Cola and Mauro reported the SP of Pt^{II} complex **11**, which forms three aggregates with remarkably different emission properties (Figure 11a).[46] Initially, kinetic nanoparticle aggregates **A** were obtained after injecting a 1,4-dioxane solution of molecularly dissolved **11** into water. These nanoparticles, which are strongly emissive due to close Pt–Pt interactions, convert into the thermodynamic species **C** within three weeks. Solvent composition-dependent as well as VT-UV/Vis and photoluminescence (PL) studies revealed a cooperative mechanism for the formation of **C** in contrast to the isodesmic growth for **A**. By adjusting the water/dioxane ratio after obtaining **A**, the energy barrier for the **A**→**C** conversion could be modulated, which allowed the process to be monitored by fluorescence confocal microscopy (Figure 11b). Surprisingly, an intermediate species **B** was observed in these experiments. The transient nature of this assembly precluded its isolation when starting from monomeric **11**. However, irradiation of **C** (λ_{exc} = 405 nm) resulted in a fast, quantitative **C**→**B** conversion.

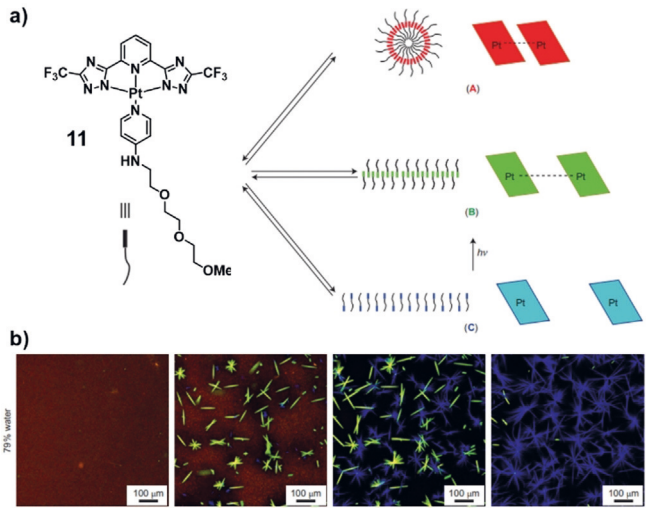

Figure 11. a) Chemical structure of Pt complex **11** and schematic representation of its self-assembly pathways. b) Fluorescence confocal microscopy images depicting the evolution (from left to right) of **A** into **B** and **C**. Adapted from Ref. [46] with permission. Copyright 2015 Springer Nature.

Sugiyasu, Takeuchi, and co-workers demonstrated that LSP is not limited to off-pathway assemblies or inactive monomers serving as the polymerization feedstock.[27] Similar to **7**, ZnPs **12** and **13** self-assemble into J-aggregate nanoparticles (NPs) through an isodesmic mechanism (Figure 12).

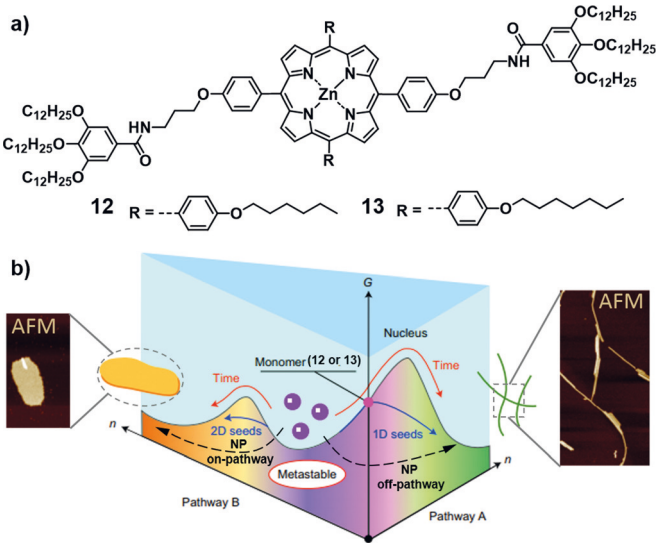

Figure 12. a) Chemical structure of ZnPs **12** and **13** as well as b) the energy landscape depicting one- and two-dimensional LSP along thermodynamic and kinetic pathways. Adapted from Ref. [27] with permission. Copyright 2016 Springer Nature.

After a lag time, the NPs propagate into 2D nanosheets (NSs). This process is accelerated by increasing the ZnP concentration, which indicates that **13**$_{NP}$ is an on-pathway intermediate in the formation of **13**$_{NS}$. Notably, this is one of the few examples of a non-hierarchical consecutive pathway. Moreover, sonication of **12**$_{NP}$ produced H-type nanofibers (NFs). This transition is, however, decelerated upon increasing the concentration. Thermodynamic analysis disclosed the fibers to be of slightly lower energy than **12**$_{NS}$, thus being the thermodynamic structure. Hence, **12**$_{NP}$ is simultaneously an on-pathway intermediate along the kinetic route and an off-pathway intermediate in the thermodynamic route. Strikingly, LSP could be performed along both pathways, thereby leading to 1D and 2D supramolecular architectures, respectively. The difference in the dimensionality of the seeds was evident from the kinetics of the seeded growth: 1D fibers propagated linearly with time, whereas the growth of the "reactive edge" in the nanosheets resulted in a sigmoidal transition. Based on the profound understanding of the energy landscape governing this system, exceptional control over this multidimensional system could be achieved (Figure 12b).

Very recently, Würthner and co-workers reported one of the most complex SP systems investigated to date. Perylene

 © 2019 The Authors. Published by Wiley-VCH Verlag GmbH & Co. KGaA, Weinheim

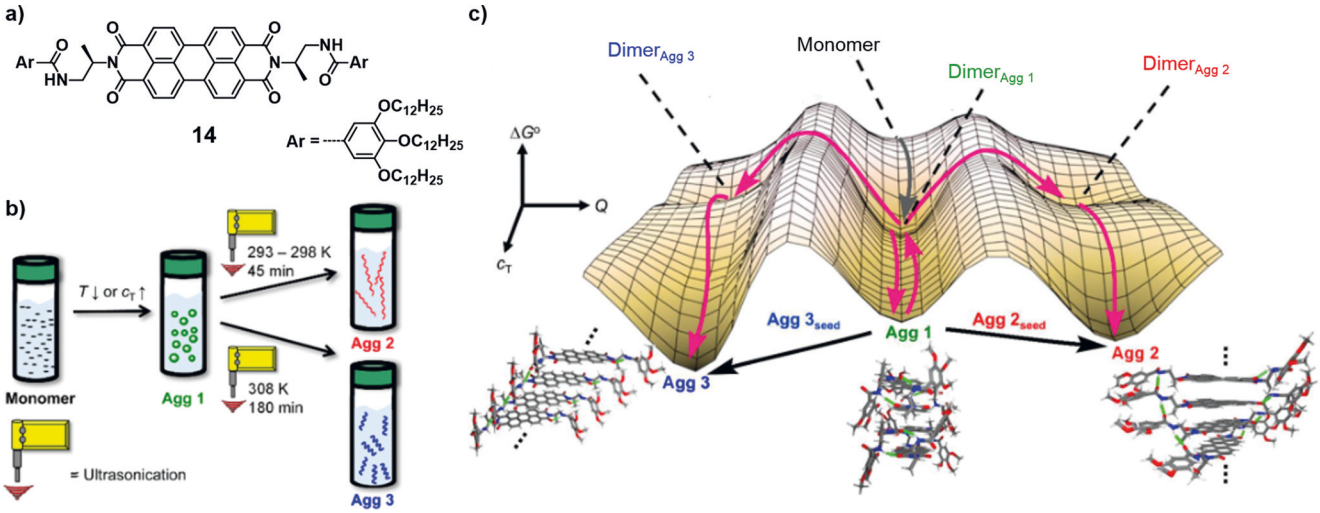

Figure 13. a) Chemical structure of PBI **14** and b) its self-assembly into three different supramolecular polymorphs **Agg 1**—**Agg 3**. c) Qualitative 3D energy landscape of **14** illustrating its SP pathways. Parameter *Q* represents the lowest-energy transformation pathway at a given concentration. Adapted from Ref. [47] with permission. Copyright 2019 American Chemical Society.

bisimide (PBI) **14** self-assembles into three supramolecular polymorphs (**Agg 1** — **Agg 3**, Figure 13a,b).[47] Upon increasing the concentration, **14** self-assembles into **Agg 1** dimers, which elongate into oligomers through an anticooperative process. The high energy barrier associated with the nucleation step for the growth of the cooperatively formed **Agg 2** + **3** prevents their formation under dilute conditions.

However, both **Agg 2** and **Agg 3** can be obtained from **Agg 1** by sonication (Figure 13b). Quantum chemical simulations starting from optimized dimer structures elucidated that both **Agg 1**→**Agg 2** and **Agg 1**→**Agg 3** transformations proceed through rearrangement of the dimers, which does not require disassembly. This unprecedented, simultaneous on-pathway nature of **Agg 1** with regard to **Agg 2** and **Agg 3** was confirmed experimentally for both transitions. Moreover, the two transformations could be induced chemically by the addition of the respective seeds to solutions of **Agg 1**. The qualitative energy landscape in Figure 13c summarizes all the characteristics of the system. It furthermore perfectly exemplifies how the precise description of the individual pathways and phenomena according to the concepts discussed in Sections 2.3–2.6 will help to fully understand and compare such highly complex systems.

3. Conclusion and Outlook

In this Minireview, we have summarized the existing concepts used to describe SP under kinetic and thermodynamic control and critically reviewed their use in the current literature. The selected examples show that careful attention has to be paid to the terminology used to describe the nature of pathways and their mutual relationship, especially in the context of pathway complexity. Furthermore, various preparation methods to access different aggregates from the same monomer as well as the corresponding energy landscapes have been outlined. It is important to note that each energy landscape is only valid for one set of final experimental conditions. However, as a result of kinetic contributions, the way to reach these conditions biases the product of SP. Nevertheless, this dependence on experimental parameters allows the polymerization outcome to be regulated (e.g switching on or off certain pathways or changing the energy landscape by changing the final conditions). We believe that this work facilitates the establishment of reliable energy landscapes for self-assembled systems and enables the generalization of current concepts in the literature. Thus, a detailed understanding of the respective energy landscape will enable the fine-tuning of the self-assembly and, in turn, the functional properties of the emerging materials.

Acknowledgements

Financial support by the MINECO of Spain (CTQ2017-82706-P) and the Comunidad de Madrid (P2018/NMT-4389) is acknowledged. Y.D. is thankful to Comunidad de Madrid for his predoctoral fellowship. G.F. thanks the European Commission (ERC-StG2016-SUPRACOP-715923). J.M. thanks the "Verband der chemischen Industrie" for his Kekulé PhD Fellowship.

Conflict of interest

The authors declare no conflict of interest.

How to cite: *Angew. Chem. Int. Ed.* **2019**, *58*, 16730–16740
Angew. Chem. **2019**, *131*, 16884–16895

[1] C. K. McLaughlin, G. D. Hamblin, H. F. Sleiman, *Chem. Soc. Rev.* **2011**, *40*, 5647–5656.
[2] a) J. M. Lehn, *Proc. Natl. Acad. Sci. USA* **2002**, *99*, 4763–4768; b) R. Breslow, *J. Biol. Chem.* **2009**, *284*, 1337–1342.

 © 2019 The Authors. Published by Wiley-VCH Verlag GmbH & Co. KGaA, Weinheim

[3] L. Brunsveld, B. J. B. Folmer, E. W. Meijer, R. P. Sijbesma, *Chem. Rev.* **2001**, *101*, 4071 – 4098.
[4] T. F. A. de Greef, M. M. J. Smulders, M. Wolffs, A. P. H. J. Schenning, R. P. Sijbesma, E. W. Meijer, *Chem. Rev.* **2009**, *109*, 5687 – 5754.
[5] L. Yang, X. Tan, Z. Wang, X. Zhang, *Chem. Rev.* **2015**, *115*, 7196 – 7239.
[6] a) T. Aida, E. W. Meijer, S. I. Stupp, *Science* **2012**, *335*, 813 – 817; b) D. N. Reinhoudt, M. Crego-Calama, *Science* **2002**, *295*, 2403 – 2407; c) D. van der Zwaag, T. F. A. de Greef, E. W. Meijer, *Angew. Chem. Int. Ed.* **2015**, *54*, 8334 – 8336; *Angew. Chem.* **2015**, *127*, 8452 – 8454; d) T. F. A. de Greef, E. W. Meijer, *Nature* **2008**, *453*, 171 – 173.
[7] D. Zhao, J. S. Moore, *Org. Biomol. Chem.* **2003**, *1*, 3471 – 3491.
[8] Z. Chen, A. Lohr, C. R. Saha-Möller, F. Würthner, *Chem. Soc. Rev.* **2009**, *38*, 564 – 584.
[9] R. B. Martin, *Chem. Rev.* **1996**, *96*, 3043 – 3064.
[10] M. M. J. Smulders, M. M. L. Nieuwenhuizen, T. F. A. de Greef, P. van der Schoot, A. P. H. J. Schenning, E. W. Meijer, *Chem. Eur. J.* **2010**, *16*, 362 – 367.
[11] a) L. Herkert, A. Sampedro, G. Fernández, *CrystEngComm* **2016**, *18*, 8813 – 8822; b) C. Rest, R. Kandanelli, G. Fernández, *Chem. Soc. Rev.* **2015**, *44*, 2543 – 2572; c) P. van der Schoot in *Supramolecular Polymers*, *2nd ed.* (Ed.: A. Ciferri), CRC Press, Hoboken, **2005**, p. 77 – 106; d) R. F. Goldstein, L. Stryer, *Biophys. J.* **1986**, *50*, 583 – 599; e) A. J. Markvoort, H. M. M. ten Eikelder, P. A. J. Hilbers, T. F. A. de Greef, E. W. Meijer, *Nat. Commun.* **2011**, *2*, 509 – 517; f) H. M. M. ten Eikelder, A. J. Markvoort, T. F. A. de Greef, P. A. J. Hilbers, *J. Phys. Chem. B* **2012**, *116*, 5291 – 5301.
[12] A. Lohr, M. Lysetska, F. Würthner, *Angew. Chem. Int. Ed.* **2005**, *44*, 5071 – 5074; *Angew. Chem.* **2005**, *117*, 5199 – 5202.
[13] K. Jyothish, M. Hariharan, D. Ramaiah, *Chem. Eur. J.* **2007**, *13*, 5944 – 5951.
[14] A. Lohr, F. Würthner, *Angew. Chem. Int. Ed.* **2008**, *47*, 1232 – 1236; *Angew. Chem.* **2008**, *120*, 1252 – 1256.
[15] M. M. Bouman, E. W. Meijer, *Adv. Mater.* **1995**, *7*, 385 – 387.
[16] J.-H. Ryu, M. Lee, *J. Am. Chem. Soc.* **2005**, *127*, 14170 – 14171.
[17] Y. Tidhar, H. Weissman, S. G. Wolf, A. Gulino, B. Rybtchinski, *Chem. Eur. J.* **2011**, *17*, 6068 – 6075.
[18] P. Jonkheijm, P. van der Schoot, A. P. H. J. Schenning, E. W. Meijer, *Science* **2006**, *313*, 80 – 83.
[19] P. A. Korevaar, C. Schaefer, T. F. A. de Greef, E. W. Meijer, *J. Am. Chem. Soc.* **2012**, *134*, 13482 – 13491.
[20] P. A. Korevaar, S. J. George, A. J. Markvoort, M. M. J. Smulders, P. A. J. Hilbers, A. P. H. J. Schenning, T. F. A. de Greef, E. W. Meijer, *Nature* **2012**, *481*, 492 – 496.
[21] P. A. Korevaar, T. F. A. de Greef, E. W. Meijer, *Chem. Mater.* **2014**, *26*, 576 – 586.
[22] A. Sorrenti, J. Leira-Iglesias, A. J. Markvoort, T. F. A. de Greef, T. M. Hermans, *Chem. Soc. Rev.* **2017**, *46*, 5476 – 5490.
[23] S. Dhiman, S. J. George, *Bull. Chem. Soc. Jpn.* **2018**, *91*, 687 – 699.
[24] E. Mattia, S. Otto, *Nat. Nanotechnol.* **2015**, *10*, 111 – 119.
[25] a) S. A. P. van Rossum, M. Tena-Solsona, J. H. van Esch, R. Eelkema, J. Boekhoven, *Chem. Soc. Rev.* **2017**, *46*, 5519 – 5535; b) S. Dhiman, A. Sarkar, S. J. George, *RSC Adv.* **2018**, *8*, 18913 – 18925; c) M. Tena-Solsona, B. Rieß, R. K. Grötsch, F. C. Löhrer, C. Wanzke, B. Käsdorf, A. R. Bausch, P. Müller-Buschbaum, O. Lieleg, J. Boekhoven, *Nat. Commun.* **2017**, *8*, 15895; d) J. Boekhoven, W. E. Hendriksen, G. J. M. Koper, R. Eelkema, J. H. van Esch, *Science* **2015**, *349*, 1075 – 1079.
[26] S. Sevim, A. Sorrenti, C. Franco, S. Furukawa, S. Pané, A. J. deMello, J. Puigmartí-Luis, *Chem. Soc. Rev.* **2018**, *47*, 3788 – 3803.
[27] T. Fukui, S. Kawai, S. Fujinuma, Y. Matsushita, T. Yasuda, T. Sakurai, S. Seki, M. Takeuchi, K. Sugiyasu, *Nat. Chem.* **2017**, *9*, 493 – 499.
[28] D. van der Zwaag, P. A. Pieters, P. A. Korevaar, A. J. Markvoort, A. J. H. Spiering, T. F. A. de Greef, E. W. Meijer, *J. Am. Chem. Soc.* **2015**, *137*, 12677 – 12688.
[29] a) L.-L. Kaj Ulrik, *Proteins and Enzymes: Lane Medical Lectures*, Stanford University Press, **1952**; b) K. D. Schwenke in *Studies in Interface Science*, *Vol. 7* (Eds.: D. Möbius, R. Miller), Elsevier, Amsterdam, **1998**, pp. 1 – 50.
[30] a) X. Wang, G. Guerin, H. Wang, Y. Wang, I. Manners, M. A. Winnik, *Science* **2007**, *317*, 644 – 647; b) T. Gädt, N. S. Ieong, G. Cambridge, M. A. Winnik, I. Manners, *Nat. Mater.* **2009**, *8*, 144 – 150; c) J. B. Gilroy, T. Gädt, G. R. Whittell, L. Chabanne, J. M. Mitchels, R. M. Richardson, M. A. Winnik, I. Manners, *Nat. Chem.* **2010**, *2*, 566 – 570; d) H. Qiu, G. Russo, P. A. Rupar, L. Chabanne, M. A. Winnik, I. Manners, *Angew. Chem. Int. Ed.* **2012**, *51*, 11882 – 11885; *Angew. Chem.* **2012**, *124*, 12052 – 12055.
[31] W. Wagner, M. Wehner, V. Stepanenko, S. Ogi, F. Würthner, *Angew. Chem. Int. Ed.* **2017**, *56*, 16008 – 16012; *Angew. Chem.* **2017**, *129*, 16224 – 16228.
[32] J. Kang, D. Miyajima, T. Mori, Y. Inoue, Y. Itoh, T. Aida, *Science* **2015**, *347*, 646 – 651.
[33] S. Ogi, K. Matsumoto, S. Yamaguchi, *Angew. Chem. Int. Ed.* **2018**, *57*, 2339 – 2343; *Angew. Chem.* **2018**, *130*, 2363 – 2367.
[34] S. Ogi, V. Stepanenko, K. Sugiyasu, M. Takeuchi, F. Würthner, *J. Am. Chem. Soc.* **2015**, *137*, 3300 – 3307.
[35] E. E. Greciano, L. Sánchez, *Chem. Eur. J.* **2016**, *22*, 13724 – 13730.
[36] J. S. Valera, R. Gómez, L. Sánchez, *Angew. Chem. Int. Ed.* **2019**, *58*, 510 – 514; *Angew. Chem.* **2019**, *131*, 520 – 524.
[37] E. E. Greciano, B. Matarranz, L. Sánchez, *Angew. Chem. Int. Ed.* **2018**, *57*, 4697 – 4701; *Angew. Chem.* **2018**, *130*, 4787 – 4791.
[38] J. S. Valera, R. Gómez, L. Sánchez, *Small* **2018**, *14*, 1702437.
[39] F. Würthner, S. Yao, U. Beginn, *Angew. Chem. Int. Ed.* **2003**, *42*, 3247 – 3250; *Angew. Chem.* **2003**, *115*, 3368 – 3371.
[40] S. Yagai, M. Yamauchi, A. Kobayashi, T. Karatsu, A. Kitamura, T. Ohba, Y. Kikkawa, *J. Am. Chem. Soc.* **2012**, *134*, 18205 – 18208.
[41] M. Hifsudheen, R. K. Mishra, B. Vedhanarayanan, V. K. Praveen, A. Ajayaghosh, *Angew. Chem. Int. Ed.* **2017**, *56*, 12634 – 12638; *Angew. Chem.* **2017**, *129*, 12808 – 12812.
[42] P. J. M. Stals, P. A. Korevaar, M. A. J. Gillissen, T. F. A. de Greef, C. F. C. Fitié, R. P. Sijbesma, A. R. A. Palmans, E. W. Meijer, *Angew. Chem. Int. Ed.* **2012**, *51*, 11297 – 11301; *Angew. Chem.* **2012**, *124*, 11459 – 11463.
[43] S. Ogi, K. Sugiyasu, S. Manna, S. Samitsu, M. Takeuchi, *Nat. Chem.* **2014**, *6*, 188 – 195.
[44] E. T. Powers, D. L. Powers, *Biophys. J.* **2008**, *94*, 379 – 391.
[45] A. Langenstroer, K. K. Kartha, Y. Dorca, J. Droste, V. Stepanenko, A. Q. Rodrigo, M. R. Hansen, L. Sánchez, G. Fernández, *J. Am. Chem. Soc.* **2019**, *141*, 5192 – 5200.
[46] A. Aliprandi, M. Mauro, L. de Cola, *Nat. Chem.* **2016**, *8*, 10 – 15.
[47] M. Wehner, M. I. S. Röhr, M. Bühler, V. Stepanenko, W. Wagner, F. Würthner, *J. Am. Chem. Soc.* **2019**, *141*, 6092 – 6107.

Manuscript received: May 8, 2019
Accepted manuscript online: July 4, 2019
Version of record online: September 30, 2019

 © 2019 The Authors. Published by Wiley-VCH Verlag GmbH & Co. KGaA, Weinheim